RSC Advances

ROYAL SOCIETY OF CHEMISTRY

www.rsc.org/advances

Mechanism of UV-assisted TiO_2/reduced graphene oxide composites with variable photodegradation of methyl orange

Zeyu LU, Guochang CHEN, Wenbin HAO, Guoxing SUN*, Zongjin LI

Department of Civil Engineering, The Hong Kong University of Science and Technology, Hong Kong, China.

Tel.: +852-9162-6614; Fax: +852-2358-1534.

* Corresponding author: Guoxing SUN; E-mail: kesun@ust.hk;

Abstract

TiO_2/reduced graphene oxide (TiO_2/rGO) composites with variable photodegradation efficiency of methyl orange (MO) were synthesized by combining TiO_2 and graphene oxide (GO) under ultraviolet (UV) irradiation. In this study, the influences of TiO_2 content and UV irradiation time on the reduction degree of GO during fabrication of the TiO_2/rGO composite were investigated and characterized by X-ray diffraction (XRD), Raman spectrum, X-ray photoelectron spectroscopy (XPS), Fourier transform infrared (FTIR) spectroscopy and Scanning electron microscope (SEM). The experimental results showed that the maximum reduction degree of GO can be achieved by controlling the weight ratio (TiO_2/GO) of 10 under 15 min UV irradiation, and the corresponding composite showed 1.71 times the higher photodegradation efficiency of MO over pure TiO_2, which results from the newly generated rGO with high electrical conductivity that decreases the recombination rate of excited electrons-holes in TiO_2. The results also demonstrated that the photodegradation efficiency of the TiO_2/rGO composite was closely related to the reduction of GO during fabrication of the composite. The more UV irradiation during fabrication of the composite, the higher reduction degree of GO, and therefore higher photodegradation efficiency of the TiO_2/rGO composite can be achieved, but excessive UV irradiation plays a negative effect on the photodegradation efficiency of the composite. Finally, the mechanism of UV-assisted TiO_2/rGO composites with variable photodegradation efficiency was proposed in terms of the reduction degree of GO.

Keywords: TiO_2/reduced graphene oxide composites; ultraviolet irradiation; reduction degree of graphene oxide, photodegradation efficiency.

1. Introduction

Photodegradation process of dye pollutants has attracted considerable attention in the last decades. Among various semiconductor photocatalysts, TiO_2 has been widely investigated and regarded as the most suitable materials in the degradation for different pollutants due to its high stability, low cost and nontoxicity [1-3]. However, the applications of TiO_2 are greatly limited by two disadvantages. On the one hand, the optical absorption of TiO_2 is constrained by the ultraviolet (UV) spectral region due to its large band gap (3.2 eV), and therefore the photodegradation of TiO_2 is only activated by UV light. On the other hand, the fast recombination rate of excited electron-holes in TiO_2 greatly retards its photocatalytic efficiency and limits its practical application [4-6]. Various attempts have been made to improve the work efficiency of TiO_2 by overcoming these shortcomings. Su et al. [7] reported that the photodegradation of methyl orange (MO) with the presence of TiO_2 nanoparticles can be improved to 1.8 times by incorporating a triboelectric nanogenerator whose generated electric field can effectively boost the separation and restrain the recombination of photo-generated electrons and holes. Zhu et al. [8] found that mesoporous TiO_2 microspheres synthesized by a facile solvothermal method showed more than twice the higher photodegradation percentages of MO than commercial TiO_2 (P25) in the same condition. Recently, many researchers also reported that combining TiO_2 with carbon nanomaterials, such as graphene and carbon nanotubes (CNTs), which has large surface area and high mobility of charge carriers [9-11], is an effective method to improve the photocatalytic activity of TiO_2.

Graphene, as a newly rising star material, has considerable interest due to its unique properties, such as excellent electrical conductivity, outstanding mechanical strength, large specific surface area and adsorption capacity [12, 13]. The combination of graphene and reduced graphene oxide (rGO) with TiO_2, not only improves the charge separation by transferring the excited electrons to graphene or rGO, but also enhances the specific surface areas of the composite for better absorbance. TiO_2/graphene or TiO_2/rGO composites, therefore, have arouse great attention for improving photodegradation efficiency of TiO_2. Wang et al. [14] fabricated TiO_2/graphene

composite by solvothermal method and the as-prepared composite showed an 80 % enhanced photodegradation of methyl orange (MO). Liang et al. [15] demonstrated that TiO_2/graphene composites produced by hydrolysis and hydrothermal treatments showed 110 % improved photodegradation efficiency over pure TiO_2. However, these fabrication methods are time-consuming and lack reproducibility due to the preparation and treatment variability.

Kamat et al. [16] proposed a facile and green way to the reduction of GO by UV-assisted TiO_2, and indicated that the newly formed rGO showed an order of magnitude decrease in the electrical resistance. However, the photodegradation property of the as-prepared TiO_2/rGO composite by UV method has not been investigated, and it still lacks a comprehensive study on the mechanism of the TiO_2/rGO composite with variable photodegradation efficiency. In addition, the matters that has arisen regarding 'how does the TiO_2 content and UV irradiation time on the photodegradation efficiency of the TiO_2/rGO composite fabricated by the UV method', or 'what is the relationship between the reduction degree of GO and the photodegradation efficiency of the corrseponding TiO_2/rGO composite' are not yet settled.

In this study, TiO_2/rGO composites with different reduction degree of GO by controlling the TiO_2 content and UV irradiation time were fabricated and investigated by XRD, Raman spectrum, FTIR, SEM and XPS techniques. The photodegradation test of methyl orange (MO) was conducted to investigate the relationship between the reduction degree of GO and the photodegradation efficiency of the TiO_2/rGO composite. The mechanism of UV-assisted TiO_2/rGO composites with variable photodegradation of MO were finally proposed in terms of the reduction of GO.

2. Experimental process

2.1 Preparation process

GO was prepared from graphite powder (Alfa-Aesar, 200 mesh) according to the modified hummer's method [17]. Graphite powder (3 g) was added to a solution containing $K_2S_2O_8$ (2 g), P_2O_5 (2 g) and concentrated H_2SO_4 (40 mL, 98 wt. %) for 6 h mixing at 80 °C. The resulting mixture was then diluted with distilled water, filtered and washed until the pH value of the rinse water became neutral. The dried graphite oxide was re-dispersed into concentrated H_2SO_4 (100

mL, 98 wt. %) in an ice bath. $KMnO_4$ (15 g) was gradually added and stirred for 2 h. The mixture was then stirred and mixed at 35 °C for another 2 h, followed by addition of 230 mL distilled water. The resultant bright yellow solution was terminated by adding 700 mL distilled water and 15 mL 30% H_2O_2, and subjected to centrifugation and carefully washing by 37 % HCl and distilled water. After immersing the as-prepared suspension in dialysis tubing cellulose membranes for 7 days, it was finally centrifuged and collected for preparing different concentrations of GO solution. In this study, the concentration of the GO solution was 1.0 mg/mL.

Varying amounts of TiO_2 and 5 mL of 1 mg/mL GO solution were firstly dissolved in 50 mL ethanol with 30 min ultrasonication to achieve homogenous dispersion. The solution was then stirred and illuminated under a 36 W UV lamp (wave crest at 254 nm) for varying periods of time in a nitrogen environment. Finally, the resultant TiO_2-rGO composite was collected by centrifugation, washed with distilled water and dried in a vacuum oven at 50 °C for 12 h. In this study, three different weight ratios of the TiO_2 to GO of 5, 10 and 20 were used to investigate the optimum weight ratio for the maximum reduction degree of GO. Then, the effect of the UV irradiation time, varying from 3 min, 7 min, 15 min, 30 min, 4 h to 12 h, on the reduction degree of GO and the photodegradation efficiency of corresponding TiO_2-rGO composites was systematically investigated.

2.2 Characterizations

XRD was conducted on the Bruker advance-D8 power diffractometer with Cu Ka radiation (λ= 0.154178 nm). Raman scattering was conducted on a Renishaw RM 3000 Micro-Raman system using a 633 nm laser source. XPS was performed with a Physical Electronics 5600 multi-technique system to investigate the carbon status of the TiO_2/rGO composite. The UV-vis diffuse reflectance spectrum (UVDRS) was obtained on a Perkin Elmer Lambda 20 UV-vis spectrophotometer. The photoluminescence (PL) spectrum was obtained on a Hitachi F4500 at an excitation wavelength of 300 nm.

2.3 Photodegradation measurement

The TiO_2/rGO composite (25 mg) was added into 50 mL of 10 mg/L methyl orange aqueous solution and magnetically stirred in the dark for 1 h to establish the adsorption-desorption equilibration. Aliquots (3 mL) were sampled from the suspension at 15 min intervals and the TiO_2-rGO composite was removed by a filter membrane (0.2 μm, Minisart). Finally, the solution was put into a quartz cell and the adsorption spectrum was measured with a UV/VIS spectroscopy (Perkin Elmer Lambda). Each test result was a mean of 3 samples.

3. Results and discussion

Figure. 1A shows the XRD pattern of TiO_2 and TiO_2/rGO composites with different weight ratios under 30 min UV irradiation. It clearly shows that the reduction of GO is not fully activated under lower weight ratio because the characteristic peak ($2\theta = 10.7°$) of the GO still occurs, as seen in curve ***b*** of Fig. 1A. With the increasing amount of TiO_2, the characteristic peak of the GO disappears in the curves ***c*** and ***d*** of Fig. 1A, and the corresponding characteristic peak of the rGO is expected to appear in the XRD patterns. However, many researchers have pointed out that the characteristic peak of the rGO generated in the reduction process cannot be seen in the XRD pattern because it is overlapped by the rutile phase of TiO_2 at around 25 ° [16-18]. In this study, the characteristic peak of the rGO in the TiO_2/rGO composite, for the first time, has been observed in the XRD pattern. Fig. 1B shows the detailed XRD patterns from 15 ° to 35 ° of TiO_2 and TiO_2/rGO composites. The sharp peak at 25 ° in curve ***a*** of Fig. 1B indicates the lattice structure of TiO_2, but it becomes broader and stronger with increasing amounts of TiO_2 in the curves ***b*** to ***d*** of Fig. 1B, resulting from the more GO reduction degree and more rGO formation. The minor changes in the XRD pattern confirms that the GO is successfully reduced to rGO. Considering the disappearance of the characteristic peak of GO in curve ***c*** of Fig. 1A and there being no big differences between curves ***c*** and ***d*** of Fig. 1B, the optimum weight ratio of TiO_2 to GO for maximum GO reduction is 10.

In order to further verify the above phenomenon, Raman scattering of different TiO_2/rGO composites was conducted, as displayed in Fig. 2. The typical bands of GO or rGO can be found at 1346 cm^{-1} (D band) and 1598 cm^{-1} (G band), and the intensity ratio of D band to G band (I_D/I_G) is proposed to be an indication of disorder in GO or rGO, originating from defects associated with vacancies, grain boundaries and amorphous carbons [19, 20]. In this study, the

value of I_D/I_G is 0.82 for GO. With the increasing amount of TiO_2, the value of I_D/I_G increases to 0.87, 1.05 and 1.06, as seen in curves ***a***, ***b*** and ***c*** of Fig. 2. The results also indicate that 10 is the optimum weight ratio for maximum GO reduction degree because the value of I_D/I_G does not increase when the weight ratio is more than 10, as shown in curves ***c*** and ***d*** of Fig. 2. The stable value of I_D/I_G indicates that there is no further transformation from sp^3 to sp^2 hybridized carbon atoms, and the reduction degree of GO cannot be further improved with the weight ratio higher than 10. The Raman results are in good consistent with the XRD results above, indicating 10 is the optimum weight ratio for maximum GO reduction.

Based on the optimum weight ratio for maximum GO reduction degree, the effect of UV irradiation time on the reduction degree of GO was further investigated by XRD, XPS and FTIR tests, and the morphology of the as-prepared TiO_2/rGO composite was characterized by the SEM technique. Fig. 3 shows the XRD patterns of TiO_2/rGO composites with optimum weight ratio of 10 but different UV irradiation times. It clearly shows that the broad peak around 25 ° becomes more and more obvious with increasing UV irradiation time, which results from the increasing reduction degree of GO. More importantly, it clearly can be seen that compared with the composite fabricated by 3 min or 7 min UV irradiation, the composite with 15 min shows a sharp increase in intensity and an obvious broader peak at 25 ° in the XRD pattern; however, there is no big difference in the XRD pattern for the composites fabricated by more than 15 min UV irradiation, revealing that no more rGO can be obtained after 15 min UV irradiation, and 15 min UV irradiation seems to be the optimum time for maximum GO reduction degree.

In order to quantitatively determine the reduction degree of GO by different UV irradiation time, XPS studies were conducted to investigate the chemical state of the carbon atoms in the TiO_2/rGO composite. Fig. 4 shows the XPS results of the GO and the TiO_2/rGO composite fabricated by 3 min, 15 min and 240 min UV irradiation. The deconvoluted C1s XPS spectrum of the sample clearly shows four types of carbon bonds, including the C-C at 284.5 eV, C-O at 286.4 eV, C=O 288.3 at eV and -COOH at 289.0 eV [21, 22]. It clearly can be seen that the relative intensity of oxygen-containing groups decrease with increasing UV irradiation time, but there is no big difference when the UV irradiation time is more than 15 min. Table 1 lists the relative content of the four carbon species. It clearly demonstrates that 15 min UV irradiation

shows the maximum GO reduction degree because there is no further obvious decreases in the relative content of the oxygen-containing groups between the composite with 15 min and 240 min UV irradiation, which means that GO cannot be further reduced with more than 15 min UV irradiation. Moreover, it also indicates that the GO cannot be fully reduced to pure graphene because the oxygen-containing carbon species still exist after the reduction process. The XPS results are in good consistent with the XRD results above.

The UVDRS spectra was conducted to investigate the optical absorption property of the TiO_2/rGO composite, as shown in Fig. 5. The neat TiO_2 exhibits the characteristic absorption at around 390 nm in the ultraviolet region, which is can be attributed to the electron transition from the valence band ($O2_p$) to the conduction band ($Ti3_d$). However, a gradual red-shift to longer wavelengths is observed for the TiO_2/rGO composites fabricated with increasing UV irradiation time, up to 15 min. The red-shift absorption is attributed to the formation of the Ti-O-C bond, which reduces the bandgap energy of the TiO_2/rGO composite. The TiO_2/rGO composites therefore show a continuously improved visible-light absorption, which is in agreement with the color change from white to grey and black, as shown in the inset of Fig. 5. More importantly, there is no obvious difference in the red-shift between the TiO_2/rGO composite fabricated by 15 min and 240 min UV irradiation, as show in the curve of *c* and *d* in Fig. 5. It also indicates no more rGO formation in the TiO_2/rGO composite after 15 min UV irradiation, which is consistent with the XRD and XPS results above.

FTIR measurements were conducted to demonstrate the reduction of GO after UV irradiation. Fig. 6displays the FTIR spectra of TiO_2, the TiO_2/rGO composite fabricated by 15 min UV irradiation and GO. In Fig. 6c, the characteristic peaks of GO at 1723 cm^{-1}, 1621 cm^{-1}, 1403 cm^{-1}, 1222 cm^{-1} and 1058 cm^{-1} indicate carboxyl or carbonyl C=O stretching, H-O-H bending band of the absorbed H_2O molecules, carboxyl O-H stretching, phenolic C-OH stretching and alkoxy C-O stretching. However, these characteristic absorption bands decrease dramatically in intensity or even disappear for the TiO_2/rGO composite (Fig. 6b), which indicates a significant reduction of GO. Moreover, the broad absorption below 1000 cm^{-1} belongs to the vibration of the Ti-O-Ti bonds in TiO_2.

Fig. 7presents typical SEM images of the as-prepared TiO_2/rGO composite. As shown in Fig. 7A, the spherical morphologies can be obtained for the TiO_2/rGO composite with a diameter range of 0.8-1.5 μm. From the high-magnified SEM image of the TiO_2/rGO composite (Fig. 7B), it is clearly seen that the TiO_2 microspheres are interconnected and wrapped by the wrinkled rGO, and the interconnection can be regarded as a 'linking-bridge' to bond the microsphere together.

Fig. 8shows the photodegradation results of MO by TiO_2 and the TiO_2/rGO composite fabricated by different UV irradiation time. The photodegradation efficiency of different composites was determined by comparing the value of C/C_0 measured after 75 min UV irradiation during the photodegradation test. The experimental results indicate that TiO_2/rGO composites fabricated by different UV irradiation time have variable photodegradation efficiency of MO, which can be summarized as the following two stages: 1) the photodegradation efficiency of the composite increases with the increasing UV irradiation time during fabrication of the composite, up to 15 min (Fig. 8, c), which shows 1.71 times the higher photodegradation efficiency over the neat TiO_2 (Fig. 8, a). The improved photodegradation efficiency result in this study is higher than many others' work results. For example, Pu et al. [23] reported that the photodegradation of the MO by the TiO_2/rGO composite via a one-pot microwave-assistant combustion method was 1.35 times higher than that of the neat TiO_2. Moreover, Wang et al. [24] demonstrated that the photodegradation of the Rhodamine B by the TiO_2/rGO films showed 1.65 times higher than that of the neat TiO_2. The mechanism of the enhanced photodegradation efficiency of the TiO_2/rGO composite fabricated by the UV irradiation method in this study is shown in Fig. 9. The TiO_2/rGO composite fabricated by 15 min UV irradiation indicates the maximum GO reduction degree, which is confirmed by the XRD, XPS and Raman results, and thus more generated rGO could participate in transferring the photogenerated electrons of TiO_2, retarding the recombination of the electron-hole pairs [14]. Because 15 min UV irradiation time during fabrication of the composite leads to the maximum reduction degree of GO, so it is reasonable that composite ***c*** in Fig. 8 shows the best photogenerated efficiency of MO. The PL spectra of samples were also measured to verify this point, as shown in Fig. 10. The PL peak around 400 nm is related to the bandgap recombination of TiO_2, while the peak around 470 nm is a result of the transition from localized surface states to the valance band of TiO_2. Compared with the neat

TiO_2, the TiO_2/rGO composites fabricated by 3 min, 7 min and 15 min show a decrease in the PL intensity, which indicates that the recombination of the electron/hole pairs can be significantly inhibited in the composite. 2) the photodegradation efficiency of the composite fabricated by more than 15 min UV irradiation (Fig. 8, d, e, f) decreases comparing with that fabricated by 15 min UV irradiation (Fig. 8, c). This is because, on the one hand, GO cannot be further reduced to rGO after 15 UV irradiation and thus it has no more contributions in hindering the electron/hole pairs recombination. On the other hand, excessive UV irradiation might cause the degradation of the left TiO_2 in the composite and thus have a negative effects on the photodegradation properties of the TiO_2/rGO composite. The experimental results indicates that the longer the UV irradiation time during fabrication of the TiO_2/rGO composite, the worse the photodegradaition efficiency of the composite. In conclude, the photodegradation efficiency of the TiO_2/rGO composite greatly depends on the GO reduction degree during fabrication of the composite, which can be strictly controlled by the TiO_2 content and UV irradiation time, and the best photodegradation efficiency of the TiO_2/rGO composite can be achieved by controlling the weight ratio of 10 under 15 min UV irradiation.

4. Conclusions

TiO_2/rGO composites with variable photodegradation efficiency of MO were synthesized by UV irradiation method. This work for the first time characterized the reduction of GO by TiO_2 under UV irradiation using XRD, Raman and XPS techniques. The relationship between GO reduction degree and the photodegradation efficiency of the corresponding TiO_2/rGO composites was preliminary established. The higher reduction degree of GO during fabrication of the TiO_2/rGO composite leads to the higher photodegradation efficiency of the composite because more excited electrons can be transferred and the recombination rate of electron-holes can be decreased. However, excessive UV irradiation during fabrication of the composite plays a negative effect on the photodegradation efficiency of the composite. The experimental results demonstrate that the photodegradation efficiency of the TiO_2/rGO composite greatly depends on the GO reduction degree during fabrication of the composite, which can be controlled by the TiO_2 content and UV irradiation time, and the highest photodegradation efficiency of the TiO_2/rGO composite can be achieved by controlling the weight ratio of 10 under 15 min UV irradiation.

Acknowledgements

Financial support from Hong Kong Research Grant Council under the Grant of 615810, China Ministry of Science and Technology under the Grant of 2015CB655100 and Information Technology of Guangzhou under the Grant of 2013J4500069 are greatly appreciated.

References

[1] Zhang C, Chaudhary U, Lahiri D, Godavarty A, Agarwal A. Photocatalytic activity of spark plasma sintered TiO 2–graphene nanoplatelet composite. Scripta Materialia. 2013;68(9):719-22.

[2] Li H, Cui X. A hydrothermal route for constructing reduced graphene oxide/TiO_2 nanocomposites: Enhanced photocatalytic activity for hydrogen evolution. International Journal of Hydrogen Energy. 2014;39(35):19877-86.

[3] Datcu A, Duta L, Perez del Pino A, Logofatu C, Luculescu C, Duta A, et al. One-step preparation of nitrogen doped titanium oxide/Au/reduced graphene oxide composite thin films for photocatalytic applications. RSC Advances. 2015;5(61):49771-9.

[4] Parayil SK, Kibombo HS, Wu C-M, Peng R, Kindle T, Mishra S, et al. Synthesis-dependent oxidation state of platinum on TiO_2 and their influences on the solar simulated photocatalytic hydrogen production from water. The Journal of Physical Chemistry C. 2013;117(33):16850-62.

[5] Shrestha KM, Sorensen CM, Klabunde KJ. MgO–TiO_2 mixed oxide nanoparticles: Comparison of flame synthesis versus aerogel method; characterization, and photocatalytic activities. Journal of Materials Research. 2013;28(03):431-9.

[6] Ajmal A, Majeed I, Malik RN, Idriss H, Nadeem MA. Principles and mechanisms of photocatalytic dye degradation on TiO2 based photocatalysts: a comparative overview. RSC Advances. 2014;4(70):37003-26.

[7] Su Y, Yang Y, Zhang H, Xie Y, Wu Z, Jiang Y, et al. Enhanced photodegradation of methyl orange with TiO2 nanoparticles using a triboelectric nanogenerator. Nanotechnology. 2013;24(29):295401.

[8] Zhu L, Liu K, Li H, Sun Y, Qiu M. Solvothermal synthesis of mesoporous TiO_2 microspheres and their excellent photocatalytic performance under simulated sunlight irradiation. Solid State Sciences. 2013;20:8-14.

[9] Zou F, Yu Y, Cao N, Wu L, Zhi J. A novel approach for synthesis of TiO_2–graphene nanocomposites and their photoelectrical properties. Scripta Materialia. 2011;64(7):621-4.

[10] Xiang Q, Yu J. Graphene-based photocatalysts for hydrogen generation. The Journal of Physical Chemistry Letters. 2013;4(5):753-9.

[11] Liu Y. Hydrothermal synthesis of TiO2-RGO composites and their improved photocatalytic activity in visible light. RSC Advances. 2014;4(68):36040-5.
[12] Geim AK, Novoselov KS. The rise of graphene. Nature materials. 2007;6(3):183-91.
[13] Lv R, Terrones M. Towards new graphene materials: doped graphene sheets and nanoribbons. Materials Letters. 2012;78:209-18.
[14] Wang Y, Li Z, He Y, Li F, Liu X, Yang J. Low-temperature solvothermal synthesis of graphene–TiO_2 nanocomposite and its photocatalytic activity for dye degradation. Materials Letters. 2014;134:115-8.
[15] Liang Y, Wang H, Casalongue HS, Chen Z, Dai H. TiO_2 nanocrystals grown on graphene as advanced photocatalytic hybrid materials. Nano Research. 2010;3(10):701-5.
[16] Williams G, Seger B, Kamat PV. TiO_2-graphene nanocomposites. UV-assisted photocatalytic reduction of graphene oxide. ACS nano. 2008;2(7):1487-91.
[17] Hummers Jr WS, Offeman RE. Preparation of graphitic oxide. Journal of the American Chemical Society. 1958;80(6):1339-.
[18] Orlita M, Faugeras C, Plochocka P, Neugebauer P, Martinez G, Maude DK, et al. Approaching the Dirac point in high-mobility multilayer epitaxial graphene. Physical Review Letters. 2008;101(26):267601.
[19] Stankovich S, Dikin DA, Piner RD, Kohlhaas KA, Kleinhammes A, Jia Y, et al. Synthesis of graphene-based nanosheets via chemical reduction of exfoliated graphite oxide. Carbon. 2007;45(7):1558-65.
[20] Ding Y, Zhang P, Zhuo Q, Ren H, Yang Z, Jiang Y. A green approach to the synthesis of reduced graphene oxide nanosheets under UV irradiation. Nanotechnology. 2011;22(21):215601.
[21] Shao L, Quan S, Liu Y, Guo Z, Wang Z. A novel "gel–sol" strategy to synthesize TiO_2 nanorod combining reduced graphene oxide composites. Materials Letters. 2013;107:307-10.
[22] Hu C, Chen F, Lu T, Lian C, Zheng S, Zhang R. Aqueous production of TiO_2–graphene nanocomposites by a combination of electrostatic attraction and hydrothermal process. Materials Letters. 2014;121:209-11.
[23] Pu X, Zhang D, Gao Y, Shao X, Ding G, Li S, et al. One-pot microwave-assisted combustion synthesis of graphene oxide–TiO 2 hybrids for photodegradation of methyl orange. Journal of Alloys and Compounds. 2013;551:382-8.
[24] Wang D, Li X, Chen J, Tao X. Enhanced photoelectrocatalytic activity of reduced graphene oxide/TiO_2 composite films for dye degradation. Chemical Engineering Journal. 2012;198:547-54.

Figure Captions

Fig. 1 (A) XRD patterns of TiO_2 and the TiO_2/rGO composite with different weight ratios of TiO_2 to GO (a) TiO_2 (b, c, d) weight ratios of 5, 10 and 20; (B) Detailed XRD patterns of TiO_2 and different TiO_2/rGO composites (a) TiO_2 (b, c, d) weight ratios of 5, 10 and 20.

Fig. 2 Raman spectra of GO and the TiO_2/rGO composite with different weight ratios of TiO_2 to GO (a) GO (I_D/I_G= 0.82) and the TiO_2/rGO composite with weight ratios of (b) 5 (I_D/I_G = 0.87) (c) 10 (I_D/I_G = 1.05) (d) 20 (I_D/I_G = 1.06). (1: 1346 cm^{-1}; 2: 1598 cm^{-1})

Fig. 3 XRD patterns of TiO_2 and the TiO_2/rGO composites with different UV irradiation times.

Fig. 4 XPS C 1s spectra of (a) GO and the TiO_2/rGO composites fabricated by (b) 3 min UV irradiation (c) 15 min (d) 240 min.

Fig. 5 UVDRS of (a) TiO_2 and the TiO_2/rGO composite fabricated with UV irradiation time of (b) 3 min; (c) 15 min and (d) 240 min.

Fig. 6 FTIR spectra of (a) TiO_2; (b) the TiO_2/rGO composite fabricated by 15 min UV irradiation and (c) GO. (1: 1723 cm^{-1}; 2: 1621 cm^{-1}; 3: 1403 cm^{-1}; 4: 1222 cm^{-1}; 5: 1058 cm^{-1})

Fig. 7 SEM images of the TiO_2/rGO composite fabricated by 15 min UV irradiation. (a) low-magnified SEM image; (b) high-magnified SEM image.

Fig. 8 Photodegradation results of MO by (a) TiO_2 and the TiO_2/rGO composite with varying UV irradiation time (b) 3 min (c) 15 min (d) 30 min (e) 4 h (f) 12 h. (C: concentration of MO at times during degradation; C_0: initial concentration of MO).

Fig. 9 Mechanism of the UV-assisted TiO_2/rGO composites with variable photodegradation efficiency. (a) Fabrication of the composite by combining TiO_2 and GO under UV irradiation; (b) Photodegradation of the MO by the as-prepared TiO_2/rGO composite).

Fig. 10 PL spectra of (a) TiO_2 and the TiO_2/rGO composite fabricated by (b) 3 min; (c) 7 min; (d) 15 min.

Figures

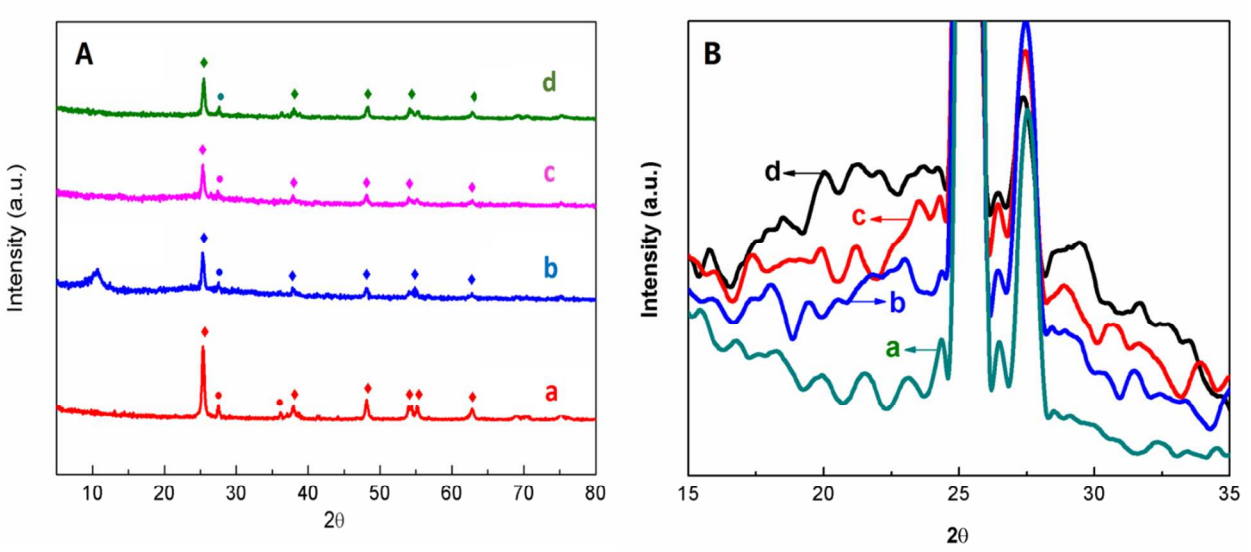

Fig. 1 (A) XRD patterns of TiO_2 and the TiO_2/rGO composite with different weight ratios of TiO_2 to GO (a) TiO_2 (b, c, d) weight ratios of 5, 10 and 20; (B) Detailed XRD patterns of TiO_2 and different TiO_2/rGO composites (a) TiO_2 (b, c, d) weight ratios of 5, 10 and 20.

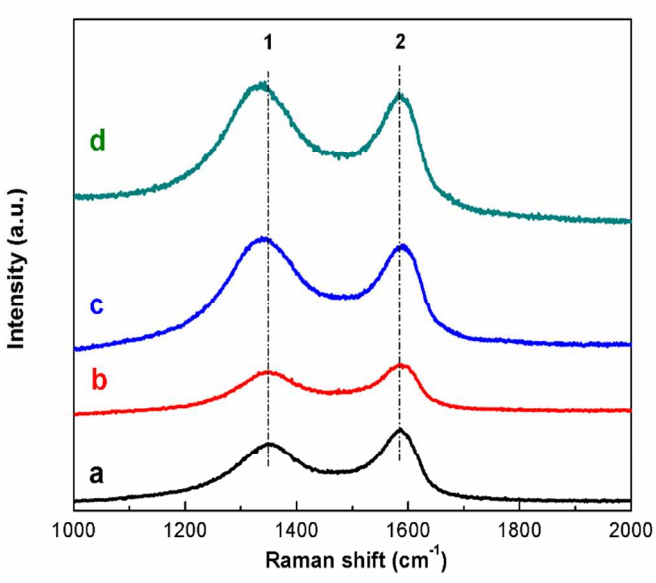

Fig. 2 Raman spectra of GO and the TiO_2/rGO composite with different weight ratios of TiO_2 to GO (a) GO (I_D/I_G = 0.82) and the TiO_2/rGO composite with weight ratios of (b) 5 (I_D/I_G = 0.87) (c) 10 (I_D/I_G = 1.05) (d) 20 (I_D/I_G = 1.06). (1: 1346 cm^{-1}; 2: 1598 cm^{-1})

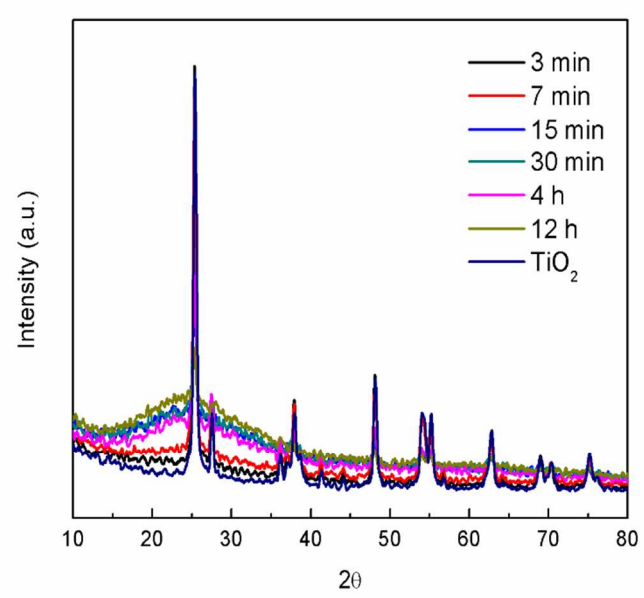

Fig. 3 XRD patterns of TiO_2 and the TiO_2/rGO composites with different UV irradiation times.

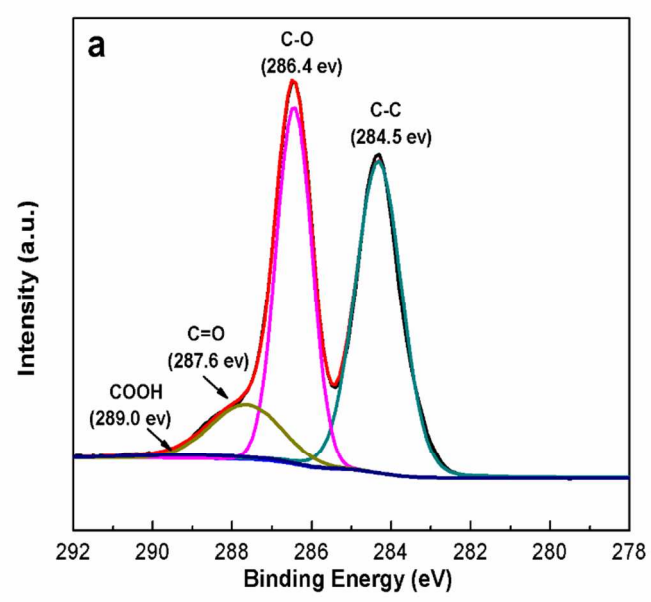

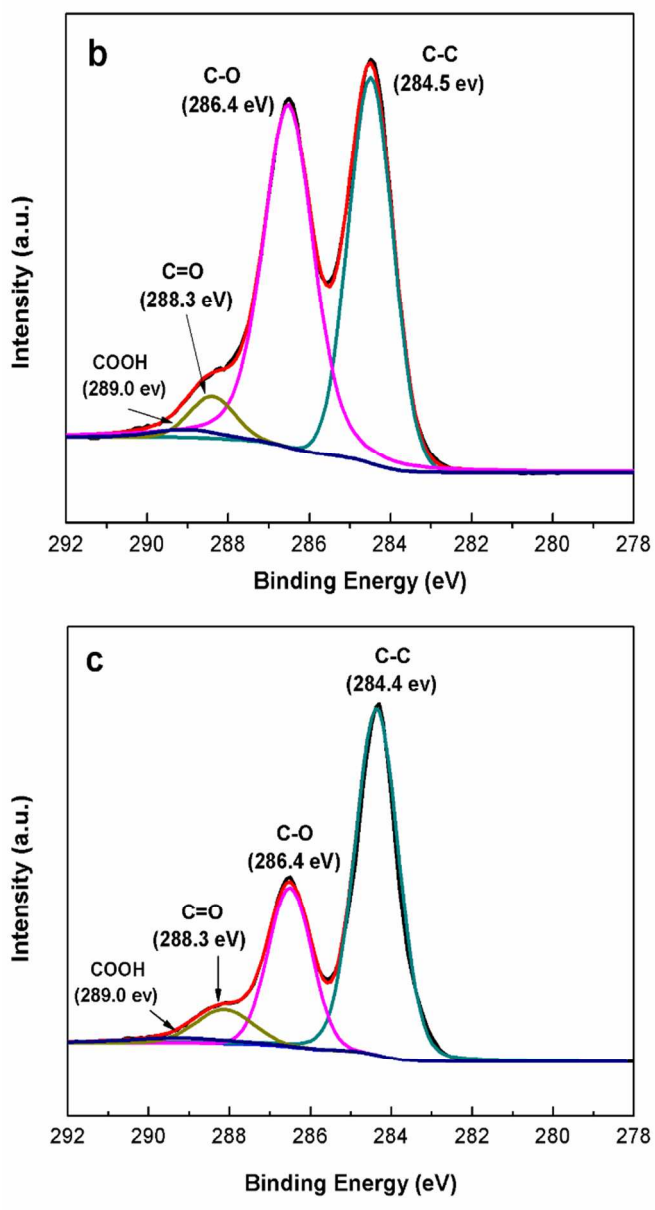

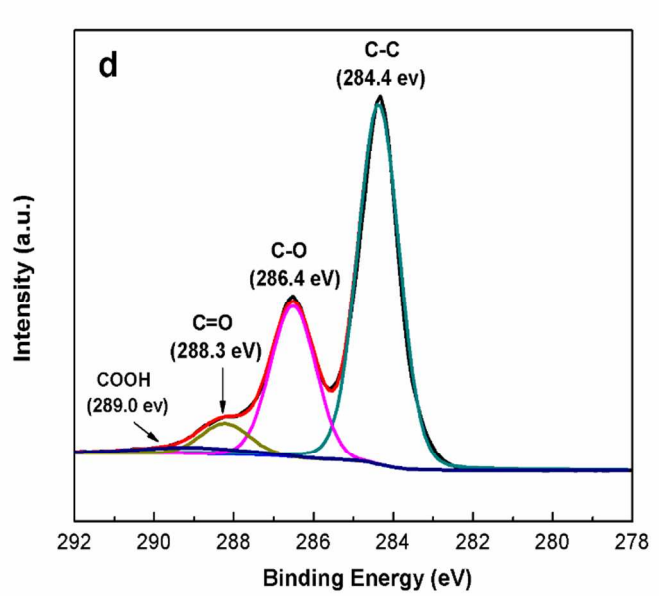

Fig. 4 XPS C 1s spectra of (a) GO and the TiO_2/rGO composites fabricated with (b) 3 min UV irradiation (c) 15 min (s) 240 min.

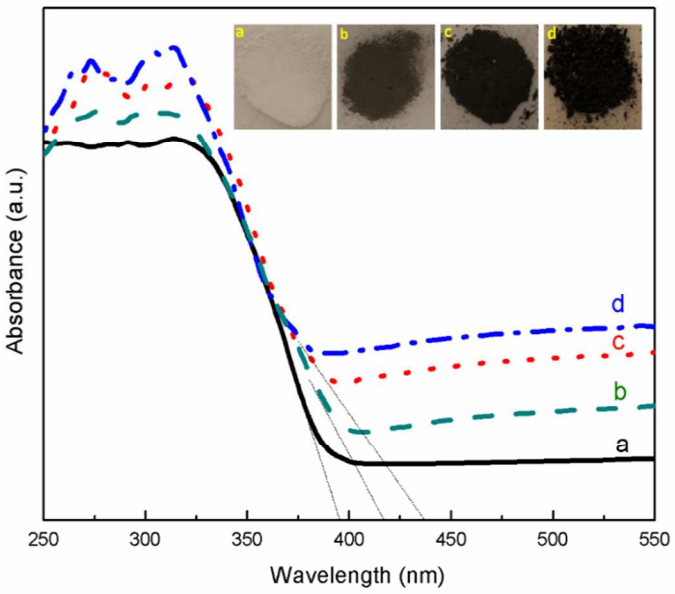

Fig. 5 UVDRS of (a) TiO_2 and the TiO_2/rGO composite fabricated with UV irradiation time of (b) 3 min; (c) 15 min and (d) 240 min.

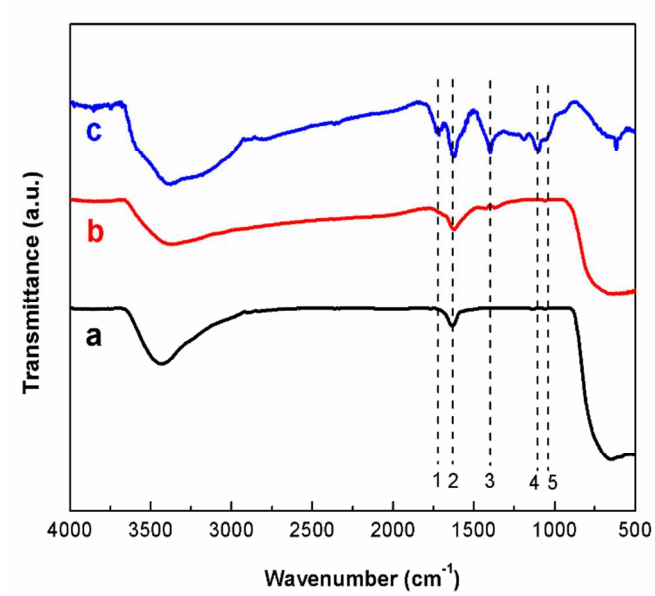

Fig. 6 FTIR spectra of (a) TiO_2; (b) the TiO_2/rGO fabricated by 15 min UV irradiation and (c) GO. (1: 1723 cm^{-1}; 2: 1621 cm^{-1}; 3: 1403 cm^{-1}; 4: 1222 cm^{-1}; 5: 1058 cm^{-1})

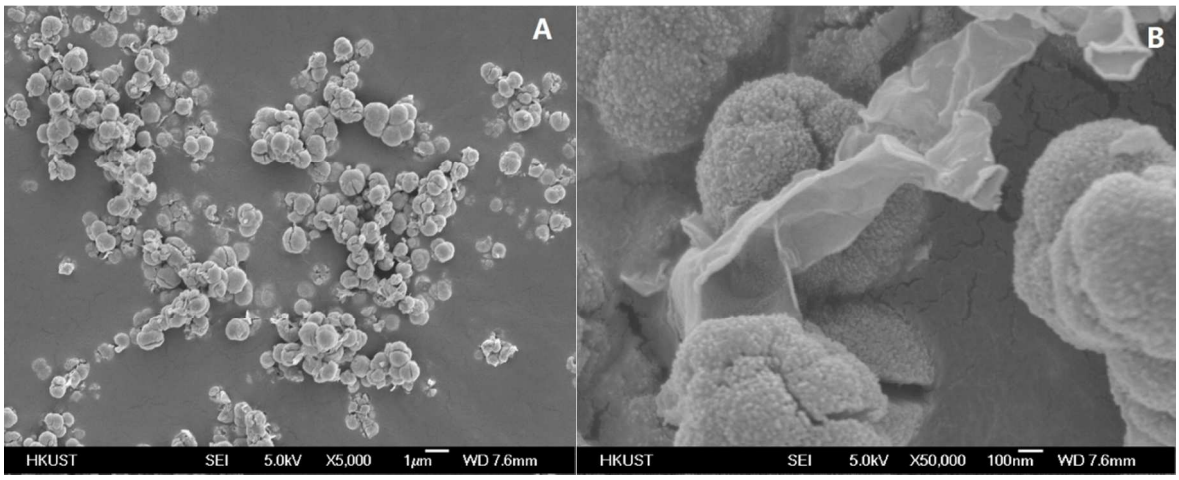

Fig. 7 SEM images of the TiO_2/rGO composite fabricated by 15 min UV irradiation. (a) low-magnified SEM image; (b) high-magnified SEM image.

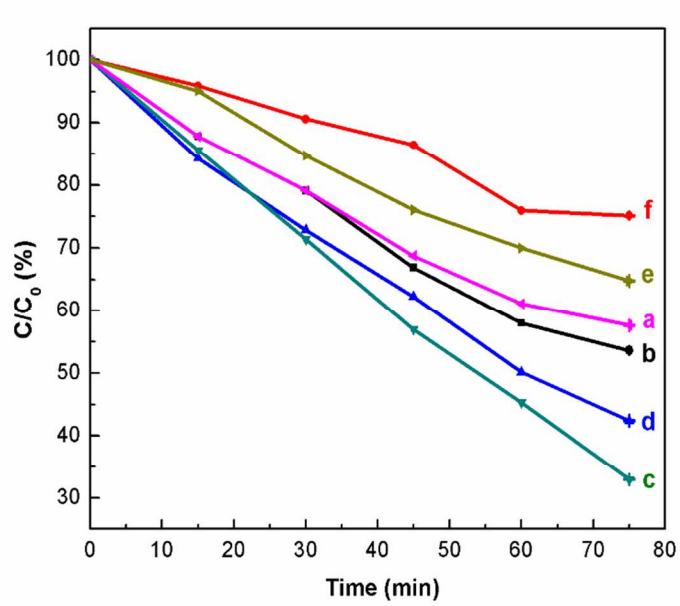

Fig. 8 Photodegradation results of MO by (a) TiO_2 and the TiO_2/rGO composite with varying UV irradiation time (b) 3 min (c) 15 min (d) 30 min (e) 4 h (f) 12 h. (C: concentration of MO at times during degradation; C_0: initial concentration of MO).

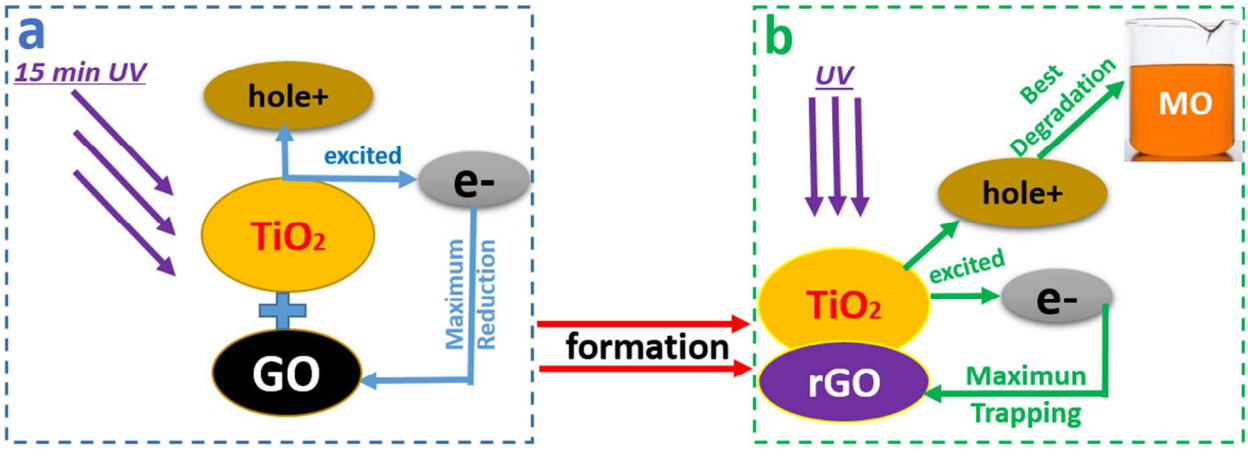

Fig. 9 Mechanism of the UV-assisted TiO_2/rGO composites with variable photodegradation efficiency. (a) Fabrication of the composite by combining TiO_2 and GO under UV irradiation; (b) Photodegradation of the MO by the as-prepared TiO_2/rGO composite).

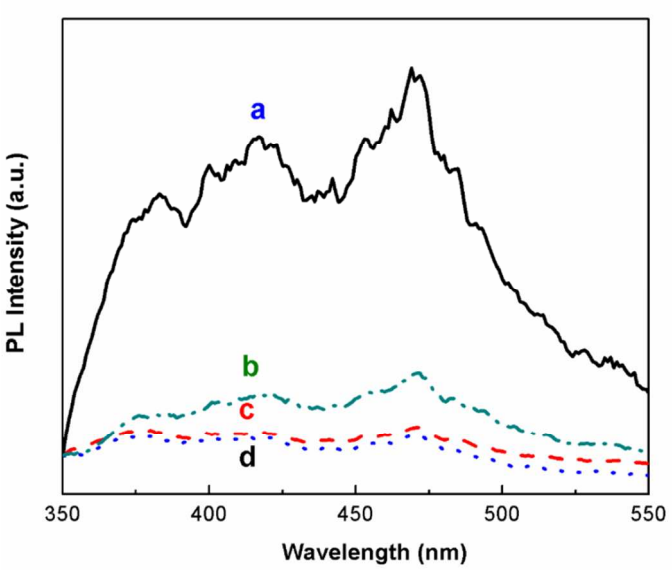

Fig. 10 PL spectra of (a) TiO_2 and the TiO_2/rGO composite fabricated by (b) 3 min; (c) 7 min; (d) 15 min.

Table

Table 1 Peak area ratios of the oxygen-containing bonds to the C-C bonds.

UV irradiation time (min)	XPS		
	$A_{C-O/C-C}$	$A_{C=O/C-C}$	$A_{COOH/C-C}$
0	1.00	0.31	0.03
3	0.81	0.23	0.02
15	0.42	0.11	0.01
240	0.40	0.10	0.01

Note: A is peak area ratios of oxygen-containing bond to C-C bond.